Title

In vivo tracking of genetically engineered, anti-HER2/neu directed natural killer cells to HER2/neu positive mammary tumors with magnetic resonance imaging

Journal

European Radiology, 15(1)

ISSN

0938-7994

Authors

Daldrup-Link, H E
Meier, R
Rudelius, M
et al.

Publication Date

2005

Peer reviewed

In-vivo Tracking of genetically engineered, anti HER2/neu directed Natural Killer Cells to HER2/neu positive Mammary Tumors with Magnetic Resonance Imaging

Purpose: To optimize labeling of the human natural killer (NK) cell line NK-92 with iron oxide based contrast agents and to monitor the in vivo distribution of genetically engineered NK-92 cells, which are directed against HER2/neu receptors, to HER2/neu positive mammary tumors with magnetic resonance (MR) imaging.

Materials and Methods: Parental NK-92 cells and genetically modified HER2/neu specific NK-92-scFv(FRP5)-zeta cells, expressing a chimeric antigen receptor specific to the tumor-associated ErbB2 (HER2/neu) antigen, were labeled with Ferumoxides and Ferucarbotran using simple incubation, lipofection, and electroporation techniques. Labeling efficiency was evaluated by MR imaging, prussian blue stains and spectrometry. Subsequently, Ferucarbotran-labeled NK-92-scFv(FRP5)-zeta (n=3) or parental NK-92 cells were intravenously injected into the tail vein of 6 mice with HER2/neu positive NIH 3T3 mammary tumors, implanted in the mammary fat pad. The accumulation of the cells in the tumors was monitored by MR imaging before and 12 and 24 hours (h) after cell injection (p.i.). MR data were correlated with histopathology.

Results: Both, the parental NK-92 and the genetically modified NK-92-scFv(FRP5)-zeta cells could be labeled with Ferucarbotran and Ferumoxides by lipofection and electroporation, but not by simple incubation. The intracellular cytoplasmatic iron oxide uptake was significantly higher after labeling with Ferucarbotran than Ferumoxides ($p<0.05$). After intravenous injection of $5*10^6$ NK-92-scFv(FRP5)-zeta cells, into tumor bearing mice, MR showed a progressive signal decline in HER2/neu positive mammary tumors at 12 and 24 h p.i.. Conversely, injection of $5*10^6$ parental NK-92 control cells, not directed against HER2/neu receptors, did not cause significant signal intensity changes of the tumors. Histopathology confirmed an accumulation of the former, but not the latter cells in tumor tissue.

Conclusion: The human natural killer cell line NK-92 can be efficiently labeled with clinically applicable iron oxide contrast agents and the accumulation of these labeled cells in murine tumors can be monitored in vivo with MR imaging. This MR cell tracking technique may be applied to monitor NK-cell based immunotherapies in patients in order to assess the presence and extend of NK-cell tumor accumulations and, thus, to determine therapy response early and non-invasively.

Key words: MR Imaging, Molecular Imaging, Iron Oxides, Cell Targeting, NK cells

Introduction:

Natural killer (NK) cells are a subpopulation of lymphocytes that play an essential role in the cell-based immune defense against virus-infected and malignant cells. Various investigators evaluated the antitumoral activity of NK cells, including the mechanisms of immunosurveillance, escape strategies of the malignant cells and risk of adverse reactions (1-3). Cancer therapy with NK cells can be performed by two approaches: Either by activation of endogenous NK cells through systemic application of cytokines (4, 5) or by adoptive transfer of ex vivo-expanded and activated autologous or donor derived NK cells (6-8). The latter approach includes the use of cytotoxic NK cell lines that are suitable for clinical use (9). The human NK cell line NK-92 (10) is highly cytotoxic against malignant cells of various origin without affecting normal human cells. Based on this selectivity, the potential of NK-92 cells for adoptive therapy is currently being investigated in phase I clinical trials. In addition to parental NK-92 cells, a genetically modified variant, termed NK-92-scFv(FRP5)-zeta expresses a chimeric antigen receptor that retargets the cytotoxic activity of NK-92 specifically to HER2 expressing cells (11). HER2 (synonymes: HER2/neu, ErbB2) is a receptor expressed at the surface of the cell membrane. HER2 overexpression has been observed in many human tumors of epithelial origin and has been linked with cancer development and progression (12, 13). In contrast to parental NK-92, NK-92-scFv(FRP5)-zeta cells specifically and efficiently lyse HER2 expressing tumor cells of various origin and, upon coinjection, markedly delay growth of HER2 positive tumors (11). However, the identification of responders and non-responders to such cell based immunotherapies still relies on the diagnosis of a decline in tumor size several weeks after cell administration. A method, which would allow to label and track the administered NK cells, could verify or disprove an accumulation of the cells in the tumor tissue and, thus, could identify responders and non-responders early after cell administration.

Currently available cell labeling techniques are based on radioactive, fluorescent or (super-)paramagnetic markers (14-21). Labeling techniques with radioactive markers provide a high sensitivity but limited spatial resolution and the risk of radiotoxic cell damage (14-17). Labeling techniques with fluorescent markers provide a high sensitivity, but limited anatomical resolution and are currently restricted to experimental applications (18, 19). Labeling techniques with contrast agents for magnetic resonance (MR) imaging have the advantage to be less toxic than radioactive and fluorescent markers and to provide an anatomical resolution at a near microscopic level in vivo (17, 20,

21). However, MR cell tracking techniques are restricted by a limited sensitivity, which requires highly efficient labeling techniques in order to load up the investigated cells with high amounts of contrast agent particles. Such optimized labeling methods have been developed before for various hematopoietic cell populations, including lymphocytes, monocytes and hematopoietc progenitor cells (17, 20-26). For non-phagocytic cell types, such labeling techniques required transfection, i.e. internalization of contrast agents into the cells with the help of liposomes, proteins or viral vectors (17, 20-25). Genetically engineered lymphocytes already underwent a transfection process in order to shuttle new genetic information into the cells. A subsequent secondary transfection, e.g. for purposes of contrast agent internalization, has a known lower efficiency than the primary transfection. Therefore, cell labeling protocols for genetically engineered cells need to be tailored and optimized to these cells.

The purpose of this study was (1) to optimize the labeling of genetically engineered NK-92-scFv(FRP5)-zeta and parental NK cells with iron oxide based MR contrast agents and (2) to monitor the accumulation of intravenously injected, iron oxide labeled NK-92-scFv(FRP5)-zeta (directed against HER2/neu receptors) and parental NK cells (directed against HER2/neu receptors) in HER2/neu positive mammary tumors with MR imaging.

Materials and Methods:

Cells and culture conditions

The continuously growing IL-2-dependent NK cell line NK-92 (23) and transduced NK-92-scFv(FRP5)-zeta cells (27, 28) expressing a chimeric antigen receptor specific to the tumor-associated ErbB2 (HER2/neu) antigen were propagated in X-VIVO 10 medium (Cambrex, Verviers, Belgium) supplemented with 5% heat-inactivated human serum and 100 units/mL IL-2 (Proleukin, Chiron, Emeryville, CA).

Prior to labeling with MR contrast agents, the cell samples were washed twice in HF/2, centrifuged, and the resultant cell pellet was resuspended with 1 ml of DMEM (Dulbecco`s Modified Eagles Medium, Gibco). The number of investigated cells was counted in a cell counter prior to each experiment.

Contrast Media and Cell Labeling Procedures

Ferumoxides (Endorem®; Laboratoire Guerbet, Aulnay-sous-Bois, France and Ferridex™; Berlex Laboratories, USA) are colloid based superparamagnetic iron oxide particles (SPIO) with an R2/R1 relaxivity ratio ($L \times mmol^{-1} \times sec^{-1}$) of 160/40 and a diameter of 120-180 nm, mean 150 nm (29-31). They consist of nonstoichiometric magnetite cores, which are covered with a dextran T-10 layer and are approved as RES-specific contrast agents in the U.S. and Europe (29-31).

Ferucarbotran (Resovist™; Schering AG, Berlin, Germany), is a new, second generation SPIO with a hydrodynamic diameter of 45-60 nm. The R1 relaxivity is 7.2 ± 0.1 l/mmol*s and the R2 relaxivity is 82.0 ± 6.2 l/mmol*s at 37°C and 1.5 T. Ferucarbotran is approved for clinical use in Europe. Physico-chemical characteristics are similar to ferumoxides, but ferucarbotran particles are covered by an anionic dextran derivative instead of a dextran layer T (29, 32).

Labeling of NK-92-scFv(FRP5)-zeta cells and parental NK-92 cells with ferumoxides or ferucarbotran was performed by simple incubation, transfection or electroporation. For comparison, control NK cells were labeled with gadopentetate dimeglumine, and additional control NK cells underwent simple incubation, transfection or electroporation with contrast agent free medium.

Simple incubation was performed by incubating samples of $1*10^6$ NK cells with Ferumoxides or Ferucarbotran at a dose of 100-300 μg Fe for variable time intervals of 2-24 hours in a humidified 37°/5% CO_2 incubator at 37° C.

Transfection was achieved by incubating $1*10^6$ NK cells with Ferumoxides or Ferucarbotran at a dose of 100 μg Fe and 20 μl of liposome formulation (Lipofectin, Life Technologies, Gibco BRL) for variable time intervals of 2-24 hours in a humidified 37°/5% CO_2 incubator at 37° C. Two to four of these unilammelar liposomes (size of 100-200 nm) associate with a single contrast agent molecule or particle, the lipid complex fuses with the cell plasma membrane and delivers the contrast agent to the cell cytosol (33).

Electroporation was performed using an electroporator (Amaxa biosystems, Köln, Germany) and a dedicated nucleofector medium for NK cells. The cells were washed once in phosphate-buffered saline, and samples of $1*10^6$ NK cells each were resuspended in 2.75 ml pre-warmed supplemented nucleofector solution. Ferucarbotran and Ferumoxides were added at a dose of 100 μg Fe. The cell suspensions were transferred to 2.0 mm electroporation cuvettes, and nucleofected with the Amaxa Nucleofector apparatus at increasing currents for 0.5-10 s. Cell concentration, contrast agent concentration and buffer volume were kept constant throughout all experiments. After electroporation, the cells were immediately suspended in 2.0 ml of complete medium, transferred to 12-well plates and allowed to recover in a humidified 37°/5% CO_2 incubator for 24 hours (34).

<u>In vitro studies:</u>

After the labeling procedure described above, the cells were washed at least three times with HEPES. Then, the cells were centrifuged and the cell pellets were evaluated by MR imaging at 1.5 T, using pulse sequence protocol described below. After completion of the imaging procedures, the cell probes were further analyzed with viability tests, spectrometry and prussian blue stains.

Cell viability was determined by the Trypan blue exclusion test and the MTT test. For the Trypan blue exclusion test, 2.5×10^5 NK cells as well as non-labeled controls were exposed to trypan blue and the relative number of non-stained, viable cells to the number of stained, non-viable cells was calculated. For the MTT test, multiple samples of 100µl cell suspension containing $5x10^4$ NK cells/ml were incubated for 4h with 10µl of MTT solution (3-(4,5-dimethylthiazole-2-yl)-2,5-diphenyl tetrazolium bromide, conc. 5mg/ml) and the development of formazan chrystals was determined by spectrometry. Formazan chrystals develop in living cells (detected by light absorbance at 550-570 nm) while dead

cells do not form formazan chrystals. These tests were performed at least three times for both cell types before and after labeling by an independent observer, who was blinded to the labeling procedure.

The iron (Fe)-concentration within iron oxides labeled cells was quantified by atomic absorption spectrometry (AAS) using a polarized Zeeman atomic absorption spectrometer (Hitachi, model Z-8200, Japan). If necessary, the cell suspensions were diluted with 0.05 M HCl. For the Fe-measurements, the spectrophotometer was set to 248.3 nm and calibrated with six standards, containing 89.55- 3582 µmol/l Fe in 0.05 M HCl. For quality-control, normal and abnormal lyphochek controls (Bio-Rad Laboratories, Munich, Germany) were used.

For prussian blue stains, samples of labeled and non-labeled NK cells were centrifuged, transferred to glass slides, fixed with Merck fixation and stained with prussian blue according to the method of Pearl to identify intracytoplasmatic iron oxide contrast agent particles.

In-vivo studies:

The study was performed according to the guidelines of the National Institutes of Health and the recommendations of the committee on animal research at our institution. $2.5–5*10^6$ NIH 3T3 HER2/neu receptor positive tumor cells (mouse sarcoma cell line) were injected into the mammary fat pad of six ten week-old female nude Balb/c-AnNCrl mice (Charles River Laboratories, Sulzfeld, Germany) with a body weight of 21 - 24 g. Tumor development and growth was monitored by daily inspection and palpation. The tumors were allowed to grow for 14-20 days to a size of 1-1.5 cm. Then, MR imaging was performed before and after injection of $5*10^6$ Ferucarbotran-labeled cells into the tail vein of the tumor bearing mice: Three mice received injections of labeled NK-92-scFv(FRP5)-zeta cells (directed against HER2/neu receptors) and three control mice received injections of labeled parental NK-92 cells (not directed against HER2/neu receptors).

All animals were anaesthetized for the cell injections with ether. Anaesthesia for MR imaging procedures was induced by an intraperitoneal injection of a combination of 0.5 mg/kg Medetomidin (Dormitor), 5 mg/kg Midazolam (Dormicum) and 0.05 mg/kg Fentanyl (Fentanyl). After completion of the imaging experiments, 2.5 mg/kg Atipamezol (Antisedan), 0.5 mg/kg Flumazenil (Anexate) and 1.2 mg/kg Naloxon (Narcanti) were given as antagonists to awake the animals. According to the veterinarians of our team, this antagonized anaesthesia provides the least impairment of the animals. After completion of the final MR imaging studies, 24 h after NK cell injection, the animals were

sacrificed by an intracardial injection of an overdose of narcoren (pentobarbital). The tumors as well as samples from liver and spleen were excised postmortem, fixed in 10% buffered formalin solution, embedded in paraffin and processed for standard histopathology (H & E staining.). In addition, anti-CD 57 immunohistochemistry stains, directed against the NK-cells, were performed to determine an NK-cell accumulation in these tissues.

Magnetic Resonance Imaging

MR imaging was performed using a clinical 1.5 Tesla MR scanner (Philips Gyroscan Intera, Best, The Netherlands) and a dedicated birdcage coil for high resolution MR imaging (Medical Advances, Milwaukee, WI, U.S.A.) with a diameter of 11 x 11 x 6 cm.

For in vitro studies, the test tubes with centrifuged cell pellets were placed into a water-containing plastic container and this container was positioned into the birdcage coil. For the in-vivo studies, the animals were placed prone into the coil. Cells and animals were evaluated with coronal T1-weighted 3D FFE 40°/25/2.7 (α/TR/TE) and coronal T2*-weighted 3D FFE 20°/25/12 (α/TR/TE)-sequences with a FOV of 100 x 80 mm, a 512^2 pixel matrix, 2 acquisitions and an effective slice thickness of 400 μm. The in-plane spatial resolution of the MR images is 200 x 150 μm. In vivo studies in mice were performed prior to as well as 12 and 24 hours after intravenous NK cell injection.

For MR data analysis, average signal intensities (SI) of cell pellets, tumors, liver and background noise were measured by operator-defined regions-of-interests (ROI). The size of the ROIs depended on the cell pellets diameter with a minimum of 10 pixels per region. The measured SI data were normalized by the background noise and expressed as signal-to-noise ratios: $SNR=SI_{tissue}/SI_{background}$. The difference in SI of the target tissues before and after injection of iron oxide-labeled NK cells was calculated as $\Delta SI = (SI_{post} - SI_{pre})$ / background noise (35).

Statistical Analysis

ΔSI data were displayed as means and standard errors of the means. To compare differences in ΔSI data between different time points after NK cell injection, an analysis of variance for repeated measurements was used. Mean data were compared using the Scheffe´s-test. Statistical significance was assigned if $p < 0.05$. All statistical computations were processed using Statview 4.1 software (Abacus, Berkeley, CA, U.S.A.).

Results:

In vitro studies:

For all investigated labeling techniques, ferucarbotran was more efficient than ferumoxides (Fig.1, Tab.1) and labeling of parental NK-92 cells was more efficient than labeling of NK-92-scFv(FRP5)-zeta cells. In parental NK-92 cells, the maximal iron oxide uptake could be achieved by adding lower concentrations of iron oxides or by shorter incubation periods as compared to the NK-92-scFv(FRP5)-zeta cells. However, the maximal achievable iron oxide uptake for both cell types was not significantly different (Tab.1, $p>0.05$). Therefore, all subsequent labeling protocols were optimized for the NK-92-scFv(FRP5)-zeta cells and then also applied to the parental NK cells in order to provide a comparable setup (Tab. 1).

Effective labeling of NK-92 cells resulted in a marked signal decline of iron oxide labeled cells on T2* weighted MR images (Fig. 1). The intracellular iron oxide uptake was quantified by spectrometry (Tab. 1) and proven by prussian blue stains (Fig. 2, 3). Simple incubation resulted in only minor labeling of cells with ferucarbotran and no detectable cell labeling with ferumoxides, while electroporation and lipofection provided an effective cell labeling with both, ferucarbotran and ferumoxides (Fig. 1).

Electroporation caused cell labeling within a few miliseconds, but reduced the viability of the cells significantly ($p<0.05$) (Fig.2), thereby necessitating additional cell culture time for cell recovery. Without electroporation, 97-98% or the investigated cells were viable, while at 48 hours after electroporation, less than 80% of the cells were viable (Fig. 2). Using different currents and exposure times, a maximum of 50-60% of the cells could be labeled with iron oxides.

Lipofection caused a linearly increasing cellular uptake of both, ferumoxides and ferucarbotran, with increasing incubation times up to 24 h. Further prolonged incubation times up to 48 h did not further increase the cellular iron uptake. Cell viability, determined by Trypan blue and MTT tests, did not change significantly with increasing incubation periods ($p>0.05$). Increasing iron oxide concentrations also increased cellular iron oxide uptake, but were inversely related to cell viability with minor, non significant impairment compared to controls ($p>0.05$; Fig.3). Lipofection with 100 μg Fe for 24 h (Ferucarbotran) resulted in labeling of 60% of the cells with a preserved viability of 92%. Lipofection with 200 μg Fe for 24 h (Ferucarbotran) resulted in labeling of 80% of the cells with slightly decreased viability of 88%. Using lipofection with ferucarbotran at a concentration of 100 μg Fe for 24 h, the

minimal number of NK-92 cells, to be detected with MR imaging, was $2.5*10^5$. Follow up studies showed a persistant labeling and a preserved viability of the cells for at least 5 days (Fig. 4).

In vivo studies:

After intravenous injection of $5*10^6$ Ferumoxtran-labeled anti HER2/neu directed NK-92-scFv(FRP5)-zeta cells into mice with implanted HER2/neu+ NIH 3T3 tumors, T2*-weighted MR images showed a marked signal decline of these tumors (Fig.5,6). This indicates an accumulation of the contrast agent labeled cells in the tumor tissue. Qualitatively, two of the tumors showed a homogenous signal decline (Fig. 5) and one of the tumors showed an inhomogenous, predominantly central and dorsal signal decline (Fig.6). Quantified tumor SNR data were significantly different after injection (p.i.) of Ferumoxtran-labeled cells compared to baseline scans before cell injection ($p<0.05$). The changes in tumor signal intensity were $\Delta SI=20.99\pm10.12$ at 12 h p.i. and $\Delta SI=29.56\pm8.56$ at 24 h p.i.. The spleen also showed a significant signal decline after cell injection ($p<0.05$) with ΔSI data of 7.09 ± 2.48 at 12 h p.i. and 7.75 ± 3.46 at 24 h p.i., apparently corresponding to a non-selective accumulation of some of the injected cells in this organ. The liver showed a minor, but not significant signal decline after cell injection ($p>0.05$; Fig. 6), indicative of lack of significant proportions of free iron oxides in the injected cell suspension. Liver ΔSI data were 2.69 ± 2.13 at 12 h p.i. and 4.22 ± 1.35 at 24 h p.i

Control studies after intravenous injection of $5*10^6$ Ferumoxtran-labeled NOT anti HER2/neu directed parental NK-92 cells into mice with implanted HER2/neu+ NIH 3T3 tumors, T2*-weighted MR images did not show any tumor signal decline (Fig.7). The corresponding tumor SNR data before and after cell injection were not significantly different ($p>0.05$). Changes in tumor MR signal were $\Delta SI = 1.81\pm0.79$ at 12 h p.i. and $\Delta SI = 3.66\pm1.45$ at 24 h p.i.. In these animals, however, a significant decline in liver and spleen signal intensity was observed after cell injection ($p<0.05$). The liver ΔSI data in this group were 6.55 ± 2.34 at 12 h p.i. and 10.58 ± 4.1 at 24 h p.i.. Spleen ΔSI data were 10.79 ± 3.35 at 12 h p.i. and 13.26 ± 3.69 at 24 h p.i.. This indicates no or only minor NK-92 cell accumulation in the tumor tissue (below the sensitivity of the MR system), but rather a non-selective cell accumulation in liver and spleen.

Corresponding immunohistochemistry stains confirmed an accumulation of anti HER2/neu directed NK-92-scFv(FRP5)-zeta cells in HER2/neu+ NIH 3T3 tumors (Fig.8 a). In accordance with the imaging findings, two tumors showed a diffuse accumulation of the anti HER2/neu directed NK-92 cells, while one tumor showed a more focal NK cell accumulation. No apparent difference in the

underlying tumor histopathology could be found to explain this variation in cell distribution in the tumor tissue. Immunohistopathologic evaluations of the controls did not show any accumulation of non-directed parental NK-92 cells in the HER2/neu+ NIH 3T3 tumors (Fig.8 b).

Discussion:

Our data showed, that genetically engineered human NK-92 cells can be labeled effectively with ferucarbotran and ferumoxides using optimized lipofection and electroporation techniques. Following intravenous injection into tumor bearing mice, the in vivo distribution and tumor accumulation of labeled cells can be tracked with MR imaging at a clinically applicable field strength of 1.5T.

In addition to be tailored to specific properties of already transfected NK cells, our technique provides potential advantages compared to previously described techniques for labeling of other cell types with radioactive, fluorescent or (super-) paramagnetic markers (14-20). Our MR labeling technique is non-invasive, easy to apply, less toxic (no radiotoxic cell damage) and provides 3D imaging data with high anatomical resolution. Since we used clinically applicable contrast agents and standard MR imaging equipment, our method is in principle suited for clinical applications.

The advantage of NK cell based immunotherapy compared to other immunotherapies, chemotherapy or irradiation is the high and selective cytotoxicity against tumor cells without toxicity against non-malignant allogeneic cells. In addition, NK cell cytotoxicity does not require sensitization and is not MHC-restricted. Based on the high intrinsic cytotoxic activity of NK-92 cells against a wide range of malignancies (1, 6, 9, 27) and the lack of toxicity and tumorigenic potential in immunodeficient SCID mice (1, 6), phase I/II clinical trials have been initiated. Preliminary results indicate that two infusions of NK-92 cells (highest total NK-92 cell dose transfused to one patient: 9.4×10^9 cells) in children and young adults with advanced cancer are well tolerated and do not lead to toxicity (9). PCR-based monitoring of NK-92 kinetics in the peripheral blood of the transfused patients revealed that a large portion of NK-92-cells apparently leave the circulation within minutes after transfusion. However, as the adoptively transfused NK-92 cells were not labeled, homing of NK-92 cells to the site of the tumor could not be confirmed in these previous clinical studies. Since NK-cell accumulation and infiltration in the tumor are crucial for the therapeutic efficacy, the MR imaging technique presented here could be of great importance for further developments of this anticancer immunotherapy. Using our MR imaging method, a non-invasive assessment of the presence and extend of NK cell accumulation in the tumor tissue can be obtained within one day after intravenous NK cell administration. This may allow more thorough longitudinal investigations of the in vivo cell biodistribution, the homing specificity of genetically engineered NK cell subtypes, potential interactions with additional chemotherapy and

reasons for treatment failures. For example, differences in therapy response between diffusely and more focally NK cell accumulating tumors, as seen in this study, may be investigated. Further applications could address variations in the effectiveness of cell based immunotherapies with different histopathologic tumor types, different tumor grades and different stages of tumor growth.

In this study, genetically engineered NK-92-scFv(FRP5)-zeta cells, which were directed against HER2/neu-receptors (11), were investigated as a model for NK-cell based immunotherapy. As a therapeutic alternative, the humanized monoclonal HER2-specific antibody Herceptin has been applied before as a monotherapy or in combination with chemotherapy protocols and provided an increased clinical benefit for a significant proportion of patients with HER2-overexpressing metastatic breast cancers (36). However, tumor responses could not be achieved in all patients with tumors expressing high HER2/neu levels. This justifies the development of alternative, potentially more effective therapeuticals, such as the immunotherapy described here, from a clinical point of view. Cytolytic effector cells, such as the NK-92-scFv(FRP5)-zeta cells, genetically modified to carry antibody-based receptors on the surface represent tailored targeting vehicles with the potential of improved tumor localization and enhanced therapeutic efficacy (27, 28). On the other hand, from the point of view of diagnostic imaging, the data presented here can be considered as a general proof-of-concept for in vivo monitoring of immunotherapies with MR imaging and may be applied to label and track other types of genetically engineered cells as well.

As shown by our data, labeling procedures cause a contrast agent particle uptake in only a fraction of the incubated cells and a cell-to-cell variability in labeling efficiency. We observed this non-even distribution of iron oxides within the cells with all of our experiments so far, i.e. with labeling procedures in various populations of hematopoietic cells, tumor cells and stem cells. This phenomenon of cell-to-cell variability in transfection efficiency has been recognized before and may be due to different metabolic activities, different stages in the cell cycle or different age of the cells as well as variances in random exposure of cells to the transfection agent-contrast agent particle complexes (37, 38).

With time after the labeling, some cells die and others divide. The internalized iron oxide particles are subsequently in part metabolized, randomely distributed between dividing cells or released by dying cells (21). Thus, our cell tracking method provides only accurate information about homing of the

labeled cells in the target tissue. MR signal intensity changes after several days may be due to intracellular iron oxides in original or subsequent generations of the cells, due to released interstitial iron or even due to iron, that was released from the originally labeled cells and then secondarily phagocytosed by local macrophages.

We recognize the following potential limitations of our study:

Cell tracking with MR imaging has a well known limited sensitivity compared to cell labeling techniques with radioactive tracers (14-17). Further studies have to show, if our labeling method is sensitive enough for potential clinical applications. The distribution volume of the injected labeled cells is obviously higher in patients than in mice. However, the volume of the investigated tumors may not be that different. Thus, in theory, $5*10^9$ labeled cells administered in humans should be eaqually visible in tumors with a size of up to 10 cm^3 as compared to $5*10^6$ labeled cells applied in our mice with 1 cm^3 tumors. Alternative labeling techniques for cell tracking with scintigraphy or PET are available as well (14-17). However, though the sensitivity of these techniques is about 1000fold higher as compared to MR, their spatial resolution is limited, radioactive decay limits follow up studies and radiotoxic cell damage could occur (14-17). MR imaging has the potential advantage of an improved, near microscopic anatomical resolution and non-invasiveness of the procedure.

Among all labeling methods, investigated in this study, electroporation caused the worst impairment of cell viability. The problem with the applied electroporator is, that the electroporation is done via certain programs, which do not allow the investigator to recognize the absolute frequency, time and type of pulses. We could only measure relative changes in duration and amount of energy between different programs of the system, we did not have the absolute data, which the company claims as their intellectual property. Further studies with other electroporator systems, which do allow a better recognition and more systematic variation and optimization of the applied pulses may provide better results.

The observed signal intensity changes of the tumor tissue resp. liver and spleen due to accumulation of iron oxides labeled cells is not only determined by the quantity of the cells but also by the compartimentalization of the contrast agent in individual cells and the distribution of the cells in the target tissue. Thus, the relationship between tissue signal intensity changes and number of accumulated cells is not linear and the number of cells, that accumulated in the tumor tissue, cannot be calculated based on our data. However, further studies could address this question and provide quantitative

estimates of the accumulated cells based on R2* measurements of labeled cells and target tissues before and after cell injection.

The iron oxide labeled NK cells showed a preserved viability up to five days after the labeling procedure and they were able to migrate and home in the tumor tissue as previously observed in non-labeled cells (27, 28). In this study, we did not perform additional investigations of the cell function before and after the labeling procedure. In previous studies, we investigated the function of hematopoietic cells more extensively and did not find any impairment of the cells due to our labeling procedure (26, 39). This is in accordance with data from the literature (17, 20, 22, 25, 40-42). The migration properties of our cells were apparently not impaired, otherwise they had not reached the tumor tissue after intravenous administration. Further studies have to proof, that the ability of the labeled NK cells to lyse tumor cells is also preserved.

In this study, the cells showed a persistant labeling and detectability by MR for at least 5 days. Further follow up studies are warranted to investigate the long term pharmacokinetics and elemination of the internalized iron oxides, which would be expected to parallel the well documented pharmacokinetics of the same iron oxide compounds after intravenous administration, i.e. the dextran coat is degraded and eliminated via the kidneys, whereas the iron oxides are distributed to the normal iron metabolism, such as heme synthesis or storage in the liver (29, 31). Of note, ferucarbotran showed an excellent safety profile in phase I-III studies (31, 32).

In summary, human natural killer cells can be labeled with MR contrast agents, that are FDA-approved or which are beeing evaluated for approval, and the in vivo distribution of these labeled cells can be depicted non-invasively using a clinical 1.5 Tesla MR scanner. This MR based NK cell tracking technique may improve our understanding of new cell based immunotherapies and may be clinically applicable to monitor NK cell homing and engraftment in human tumors.

Acknowledgement:

This work was supported by an ECR foundation grant

References:

1. Tam Y K, Miyagawa B, Ho V C, Klingemann, H. G. (1999) Immunotherapy of malignant melanoma in a SCID mouse model using the highly cytotoxic natural killer cell line NK-92. J Hematother 8: 281-290.

2. Raulet DH, Vance RE, McMahon CW (2001) Regulation of the natural killer cell receptor repertoire. Annu Rev Immunol19:291-330.

3. Whiteside TL (1998) Immune cells in the tumor microenvironment. Mechanisms responsible for functional and signaling defects. Adv Exp Med Biol 451:167-71.

4. Mulatero CW, Penson RT, Papamichael D, Gower NH, Evans M, Rudd RM (2001) A phase II study of combined intravenous and subcutaneous interleukin-2 in malignant pleural mesothelioma. Lung Cancer 31(1): 67-72.

5. Maraninchi D, Vey N, Viens P, Stoppa AM, Archimbaud E, Attal M, Baume D, Bouabdallah R, Demeoq F, Fleury J, Michallet M, Olive D, Reiffers J, Sainty D, Tabilio A, Tiberghien P, Brandely M, Hercend T, Blaise D (1998): A phase II study of interleukin-2 in 49 patients with relapsed or refractory acute leukemia. Leuk Lymphoma 31(3-4): 343-9.

6. Yan Y, Steinherz P, Klingemann H G, Dennig D, Childs B H, McGuirk J, O'Reilly R J (1998) Antileukemia activity of a natural killer cell line against human leukemias. Clin Cancer Res 4: 2859-2868.

7. Nagayama H, Takahashi S, Takahashi T et al. (1999) IL-2/LAK therapy for refractory acute monoblastic leukemia relapsing after unrelated allogeneic bone marrow transplantation. Bone Marrow Transplant 23:183-185

8. Kimoto Y, Tanaka T, Tanji Y, Fujiwara A and Taguchi T (1994) Use of human leukocyte antigen-mismatched allogeneic lymphokine-activated killer cells and interleukin-2 in the adoptive immunotherapy of patients with malignancies. Biotherapy 8:41-50

9. Tonn T, Becker S, Esser R, Schwabe D, Seifried E (2001) Cellular immunotherapy of malignancies using the clonal natural killer cell line NK-92. J Hematother Stem Cell Res 10: 535-544.

10. Gong JH, Maki G, Klingemann HG (1994) Characterization of a human cell line (NK-92) with phenotypical and functional characteristics of activated natural killer cells
Leukemia 8(4): 652-8.

11. Uherek C, Tonn T, Uherek B, Becker S, Schnierle B, Klingemann H.-G, Wels W (2002) Retargeting of NK-cell cytolytic activity to ErbB2 expressing tumor cells results in efficient and selective tumor cell destruction. Blood 100: 1265-1273

12. Klapper LN, Kirschbaum MH, Sela M, Yarden Y (2000) Biochemical and clinical implications of the ErbB/HER signaling network of growth factor receptors. Adv Cancer Res 77:25-79.

13. Olayioye MA, Neve RM, Lane HA, Hynes NE (2000) NEW EMBO MEMBERS' REVIEW: The ErbB signaling network: receptor heterodimerization in development and cancer. Embo J 19:3159-3167

14. Fawwaz R, Oluwole T, Wang N, Kuromoto N, Iga C, Hardy M, Alderson P (1985) Biodistribution of radiolabeled lymphocytes. Radiology 155:483-486.

15. Melder RJ, Brownell AL, Shoup TM, Brownell GL, Jain RK (1993) Imaging of activated natural killer cells in mice by positron emission tomography: preferential uptake in tumors. Cancer Res 15;53(24): 5867-71.

16. Adonai N, Nguyen KN, Walsh J, Iyer M, Toyokuni T, Phelps ME, McCarthy T, McCarthy DW, Gambhir SS (2002) *Ex vivo* cell labeling with 64Cu–pyruvaldehyde-bis(*N*4-methylthiosemicarbazone) for imaging cell trafficking in mice with positron-emission tomography. Proc Natl Acad Sci U S A. 2002 March 5; 99 (5): 3030–3035

17. Moore A, Grimm J, Han B, Santamaria P (2004) Tracking the recruitment of diabetogenic CD8+ T-cells to the pancreas in real time. Diabetes. 53(6):1459-66.

18. Oostendorp RA, Ghaffari S, Eaves CJ (2000) Kinetics of in vivo homing and recruitment into cycle of hematopoietic cells are organ-specific but CD44-independent. Bone Marrow Transplant 26(5): 559-66.

19. *Daldrup-Link HE*, Rudelius M, Metz S, Piontek G, Settles M, Pichler B, Heinzmann U, Weinmann HJ, Schlegel J, Link TM, Rummeny EJ, Oostendorp RAJ (2004) Stem cell tracking with Gadophrin-2 – a trifunctional contrast agent for MR imaging, optical imaging and fluorescence microscopy. Eur J Nucl Med Mol Imaging May 11 [Epub ahead of print]

20. Lewin M, Carlesso N, Tung C-H, Tang X-W, Cory D, Scadden D, Weissleder R (2000) Tat peptide-derivatized magnetic nanoparticles allow in vivo tracking and recovery of progenitor cells. Nature Biotechnology 18:410-414.

21. Daldrup-Link HE, Rudelius M, Piontek G, Metz S, Bräuer R, Debus G, Corot C, Schlegel J, Link TM, Peschel C, Rummeny EJ, Oostendorp RAJ (2004) Migration of iron oxide labeled human hematopoietic progenitor cells in a xenotransplant model: in vivo monitoring using clinical magnetic resonance imaging equipment. Radiology in press

22. Smirnov P, Gazeau F, Lewin M, Bacri JC, Siauve N, Vayssettes C, Cuenod CA, Clemont O (2004) In vivo cellular imaging of magnetically labeled hybridomas in the spleen with a 1.5 T clinical MR system. Magn Reson Med 52(1):73-79.

23. Weissleder R, Cheng H, Bogdanova A, Bogdanov A (1997) Magnetically labeled cells can be detected by MR imaging. J Magn Reson Imaging 7: 258-263.

24. Schoepf U, Marecos E, Melder R, Jain R, Weissleder R (1998) Intracellular magnetic labeling of lymphocytes for in vivo trafficking studies. BioTechniques 24: 642-651.

25. Yeh T, Zhang W, Ildstad S and Ho C (1995) In vivo dynamic MRI tracking of rat T-cells labeled with superparamagnetic iron oxide particles. Magn Res Med 33:200-208.

26. Metz S, Bonaterra G, Rudelius M, Settles M, Rummeny EJ, Daldrup-Link HE (2004) Capacity of Human Monocytes to phagocytose approved iron oxide MR contrast agents. Accepted for publication in Eur Radiol

27. Klingemann H, Wong E and Maki G. A cytotoxic NK-cell line (NK-92) for ex vivo purging of leukemia from blood (1996) Biol Blod Marrow Transplant 2:68-75.

28. Uherek C, Groner B, Wels W (2001) Chimeric antigen receptors for the retargeting of cytotoxic effector cells. J Hematother Stem Cell Res 10: 523-534

29. Weissleder R (1994) Liver MR imaging with iron oxides: toward consensus and clinical practice. Radiology 193(3): 593-5.

30. Jung CW. Surface properties of superparamagnetic iron oxide MR contrast agents: ferrumoxides, ferrumoxtran, ferrumoxisil. Magn Res Imag 1995;13:675-691.

31. Wang YX, Hussain SM, Krestin GP (2001) Superparamagnetic iron oxide contrast agents: physicochemical characteristics and applications in MR imaging. Eur Radiol 11(11):2319-31.

32. Reimer P, Balzer T (2003) Ferucarbotran (Resovist): a new clinically approved RES-specific contrast agent for contrast-enhanced MRI of the liver: properties, clinical development, and applications. Eur Radiol 13(6):1266-76.

33. Felgner P, Gadek T, Holm M et al (1987) Lipofectin: a highly efficient, lipid mediated DNA-transfection procedure. Proc Natl Acad Sci USA 84: 7413-7417

34. Maasho K, Marusina A, Reynolds NM, Coligan JE and Borrego F (2004) Efficient gene transfer into the human natural killer cell line, NKL, using the amaxa nucleofection system. Journal of Immunological Methods 284:133-140.

35. Wolff S and Balaban R (1997) Assessing contrast on MR images. Radiology 202:25-29.

36. Vogel CL, Cobleigh MA, Tripathy D, Gutheil JC, Harris LN, Fehrenbacher L, Slamon DJ, Murphy M, Novotny WF, Burchmore M, Shak S, Stewart SJ, Press M (2002) Efficacy and safety of trastuzumab as a single agent in first-line treatment of HER2-overexpressing metastatic breast cancer. J Clin Oncol 20:719 –726

37. Lai JC, Yuan C, Thomas JL (2002) Single-cell measurements of polyamidoamine dendrimer binding. Ann Biomed Eng 30(3):409-16

38. Ruihua C, Greene EL, Collinsworth G, Grewal JS, Houghton O, Zeng H, Garnovskaya M, Paul RV, Raymond JR (1999) Enrichment of transiently transfected mesangial cells by cell sorting after cotransfection with GFP. Am. J. Physiol. 276 (Renal Physiol. 45): F777–F785.

39. Daldrup-Link HE, Rudelius M, Oostendorp RAJ, Settles M, Piontek G, Metz S, Heinzmann U, Rummeny EJ, Schlegel J, Link TM (2003) Targeting of Hematopoietic Progenitor Cells with MR Contrast Agents. Radiology 228: 760-767

40. Arbab AS, Bashaw LA, Miller BR, Jordan EK, Bulte JW, Frank JA (2003) Intracytoplasmic tagging of cells with ferumoxides and transfection agent for cellular magnetic resonance imaging after cell transplantation: methods and techniques. Transplantation 15;76(7):1123-30.

41. Bulte JW, Douglas T, Witwer B, Zhang SC, Strable E, Lewis BK, Zywicke H, Miller B, van Gelderen P, Moskowitz BM, Duncan ID, Frank JA (2001) Magnetodendrimers allow endosomal magnetic labeling and in vivo tracking of stem cells. Nat Biotechnol 19(12):1141-7.

42. van den Bos EJ, Wagner A, Mahrholdt H, Thompson RB, Morimoto Y, Sutton BS, Judd RM, Taylor DA (2004) Improved efficacy of stem cell labeling for magnetic resonance imaging studies by the use of cationic liposomes. Cell Transplant 12(7):743-56.

Tables and Figures:

Table 1) Cellular iron content before and after labeling with iron oxide contrast agents as determined by spectrometry. For each labeling procedure, results of optimized protocols with maximal iron oxide uptake and minimally impaired cell viability are listed.

Fig.1) MR images of centrifuged NK-92 cell pellets in test tubes. Electroporation and transfection with iron oxide contrast agents results in a strong T2*-effect of the investigated cells. The same methods can be also applied for cell labeling with Gd-DTPA.

Fig.2) Electroporation of NK-92 cells with Ferucarbotran shows limited labeling efficiencies and impairment of cell viability as determined by the Trupan blue exclusion test.

Fig.3) Transfection with Ferucarbotran shows highly efficient cellular iron uptake, subsequent strong T2*-effect of labeled cells and preserved cell viability, determined by the Trupan blue exclusion test.

Fig.4) Follow up MR images after transfection of NK-92 cells with Ferucarbotran (100 g Fe, 24h) show a persistant T2* effect of the labeled cells for 5 days.

Fig.5) T2*weighted FFE MR images show a high signal intensity of HER2/neu+ NIH 3T3 tumors before cell injection (arrows) and a marked signal decline 24 hours after injection of Ferucarbotran-labeled anti-HER2/neu directed NK-92-scFv(FRP5)-zeta cells cells. (* heat cushion).

Fig.6) T2*weighted FFE MR images of another HER2/neu+ NIH 3T3 tumor show an inhomogenous decline in signal intensity after injection of Ferucarbotran-labeled anti-HER2/neu directed NK-92-scFv(FRP5)-zeta cells cells, apparently indicating a more focal cell accumulation in the tumor tissue. The spleen also shows a signal decline, indicative of non-selective accumulation of some of the injected cells in this organ. Of note, the liver does not show any signal decline after injection of iron oxide labeled cells, excluding the presence of relevant amounts of free contrast agent in the injected cell suspension.

Fig.7) T2*weighted FFE MR images of HER2/neu+ NIH 3T3 tumors show no change in signal intensitybefore and after injection of non-specific, NOT anti-HER2/neu directed parental NK-92 cells. But liver and spleen show a signal decline, indicative of a non-specific cell accumulation in these organs.

Fig.8) Anti-CD 57 immunohistochemistry stains, directed against the NK-cells. In A, a HER2/neu+ NIH 3T3 tumor 24 h after injection anti-HER2/neu directed NK-92-scFv(FRP5)-zeta cells shows accumulated positively stained cells (some marked with arrows) in the tumor tissue. In B, a control

HER2/neu+ NIH 3T3 tumor 24 h after injection of NOT anti-HER2/neu directed parental NK-92 cells does not show any cell accumulation in the tumor tissue.

10^6 NK-92 cells	controls	ferucarbotran	ferumoxides
simple incubation (100 μg Fe/24 h)			
parental NK-92 cells	**0.001±0.002 μg Fe**	**0.81±0.44 μg Fe**	**0.01±0.002 μg Fe**
NK-92-scFv(FRP5)-zeta cells	**0.001±0.004 μg Fe**	**0.76±0.50 μg Fe**	**0.02±0.002 μg Fe**
Electroporation (100 μg Fe)			
parental NK-92 cells	**0.002±0.005 μg Fe**	**2.53±0.62 μg Fe**	**1.32±0.48 μg Fe**
NK-92-scFv(FRP5)-zeta cells	**0.004±0.005 μg Fe**	**2.36±0.49 μg Fe**	**1.18±0.42 μg Fe**
Transfection (100 μg Fe/24 h)			
parental NK-92 cells	**0.001±0.002 μg Fe**	**2.86±0.80 μg Fe**	**1.55±0.65 μg Fe**
NK-92-scFv(FRP5)-zeta cells	**0.002±0.002 μg Fe**	**2.94±0.66 μg Fe**	**1.37±0.48 μg Fe**

Table 1)

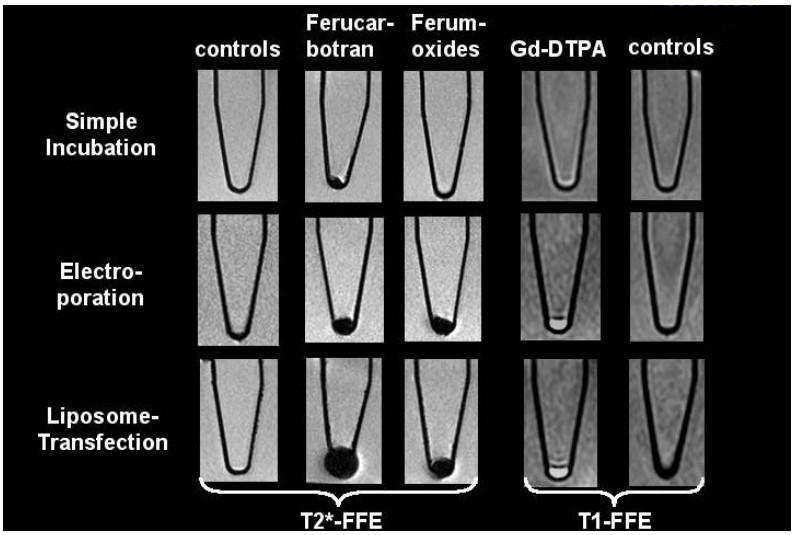

Fig.1)

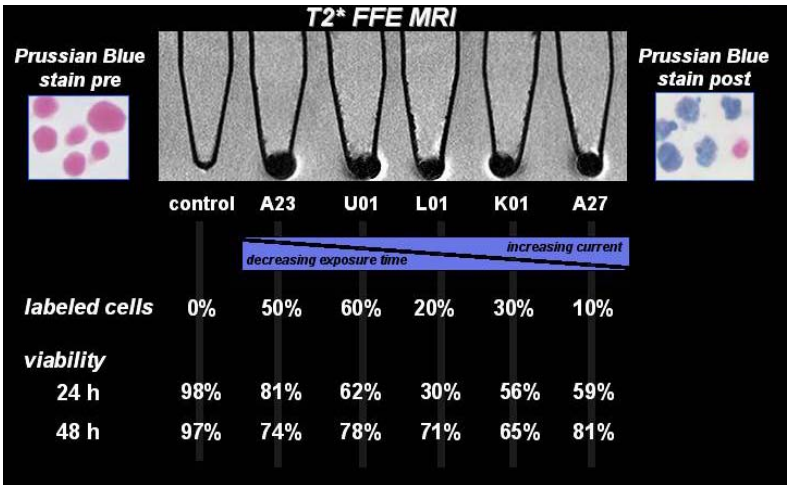

Fig.2)

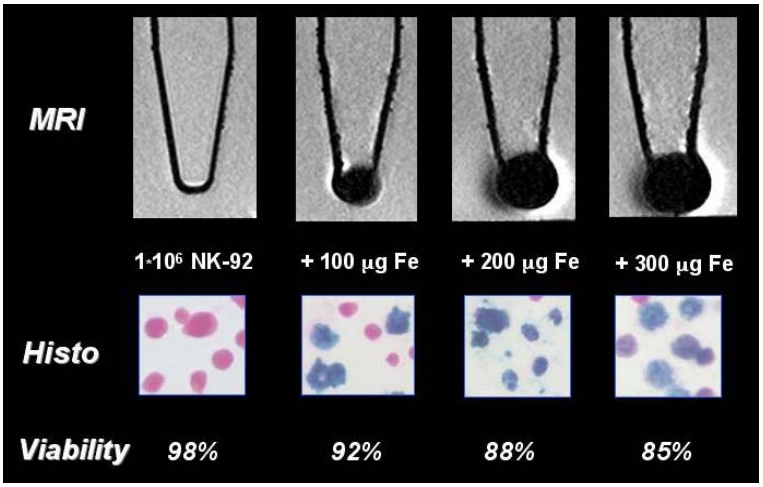

Fig.3)

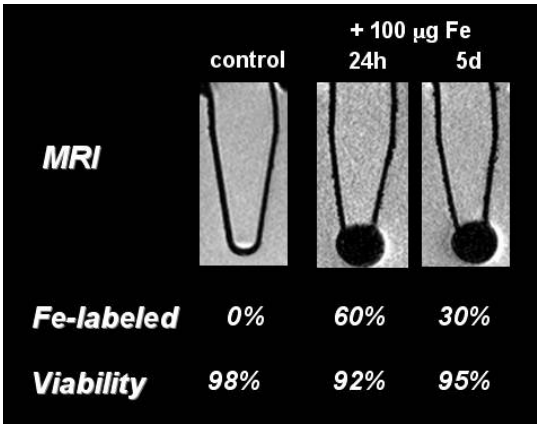

Fig.4)

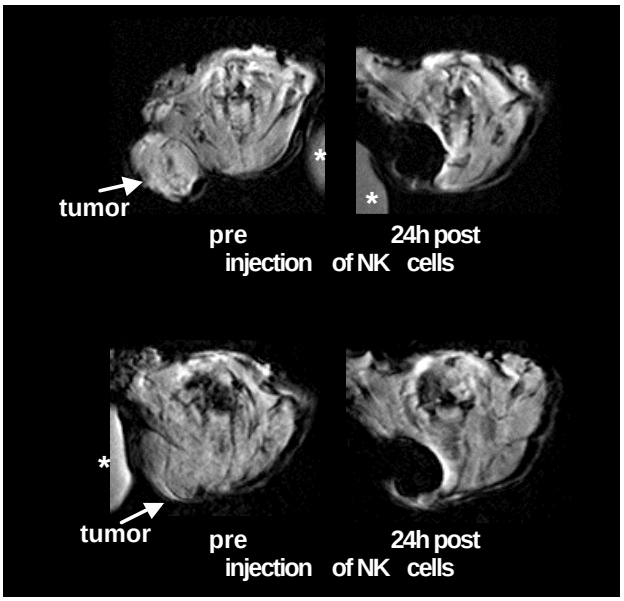

Fig.5)

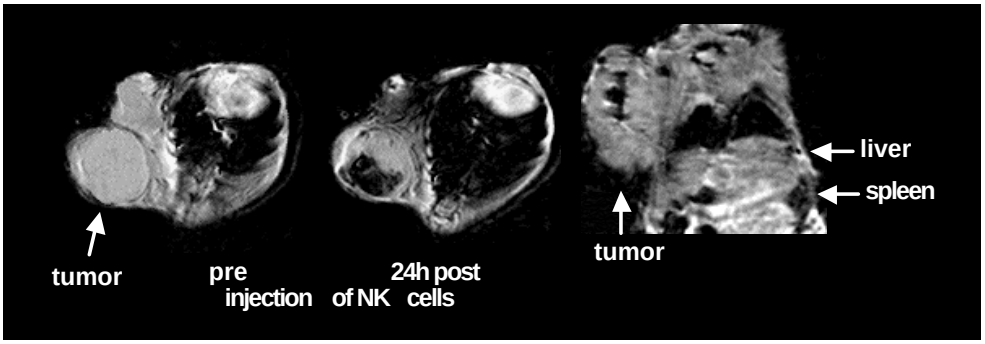

Fig.6)

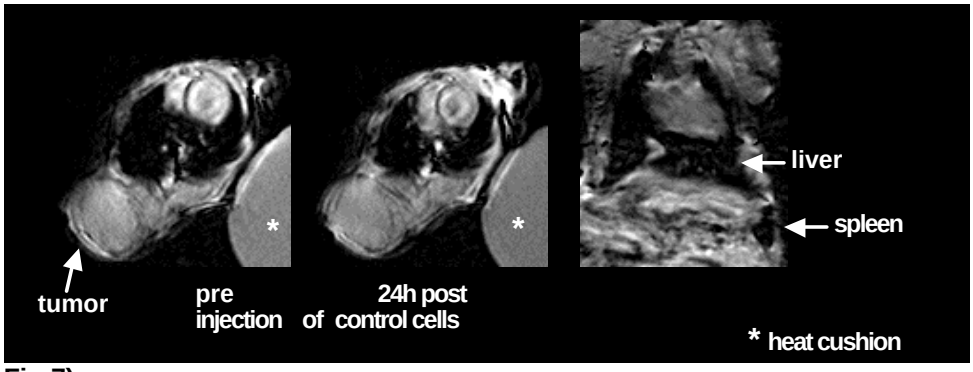

Fig.7)

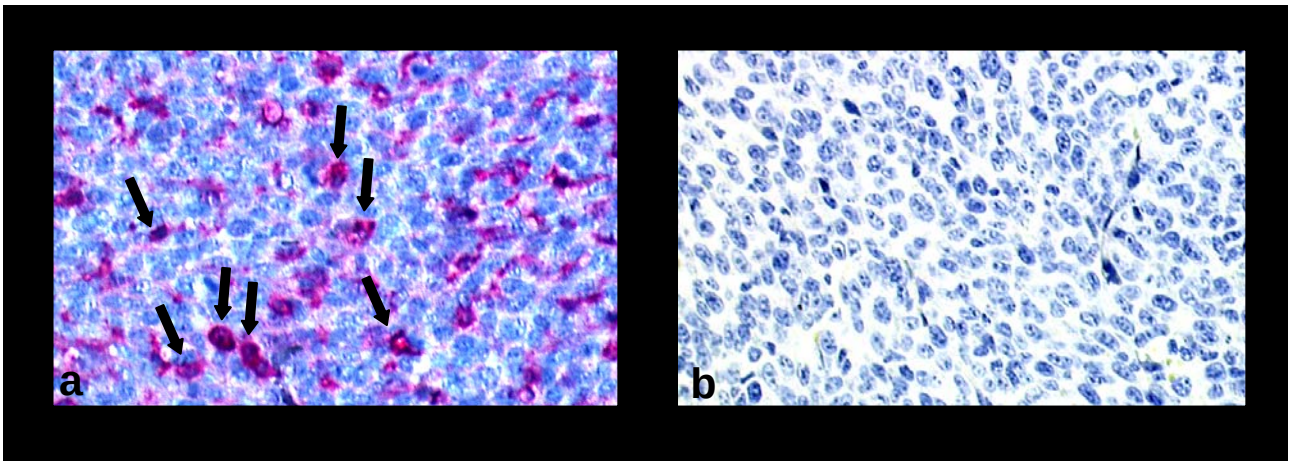

Fig.8)